OFFICE OF NAVAL RESEARCH

GRANT NOOO14-89-J-1178

R&T Code 413Q001-05

TECHNICAL REPORT NO. #40

Infrared Rotating Analyzer Ellipsometry: Calibration And Data Processing

by

V. A. Yakovlev , M. Li and E. A. Irene
Department of Chemistry, CB# 3290
University of North Carolina
Chapel Hill, NC 27599-3290

Submitted to the
Journal of Optical Society American A

SECURITY CLASSIFICATION OF THIS PAGE

REPORT DOCUMENTATION PAGE

1a. REPORT SECURITY CLASSIFICATION unclassified	1b. RESTRICTIVE MARKINGS
2a. SECURITY CLASSIFICATION AUTHORITY	3. DISTRIBUTION/AVAILABILITY OF REPORT Approved for public release; distribution unlimited.
2b. DECLASSIFICATION/DOWNGRADING SCHEDULE	
4. PERFORMING ORGANIZATION REPORT NUMBER(S) Technical Report #40	5. MONITORING ORGANIZATION REPORT NUMBER(S)
6a. NAME OF PERFORMING ORGANIZATION UNC Chemistry Department 6b. OFFICE SYMBOL (If applicable)	7a. NAME OF MONITORING ORGANIZATION Office of Naval Research (Code 413)
6c. ADDRESS (City, State and ZIP Code) CB# 3290, Venable Hall University of North Carolina Chapel Hill, NC 27599-3290	7b. ADDRESS (City, State and ZIP Code) Chemistry Program 800 N. Quincy Street Arlington, Virginia 22217
8a. NAME OF FUNDING/SPONSORING ORGANIZATION Office of Naval Research 8b. OFFICE SYMBOL (If applicable)	9. PROCUREMENT INSTRUMENT IDENTIFICATION NUMBER Grant #N00014-89-J-1178
8c. ADDRESS (City, State and ZIP Code) Chemistry Program 800 N. Quincy Street, Arlington, VA 22217	10. SOURCE OF FUNDING NOS. PROGRAM ELEMENT NO. / PROJECT NO. / TASK NO. / WORK UNIT NO
11. TITLE (Include Security Classification) INFRARED ROTATING ANALYZER ELLIPSOMETRY: CALIBRATION AND DATA PROCESSING	
12. PERSONAL AUTHOR(S) V. A. Yakovlev*, M. Li and E.A. Irene	
13a. TYPE OF REPORT Interim Technical 13b. TIME COVERED FROM _____ TO _____	14. DATE OF REPORT (Yr., Mo., Day) November 1991 15. PAGE COUNT 28
16. SUPPLEMENTARY NOTATION Journal of Optical Society American A	
17. COSATI CODES FIELD / GROUP / SUB. GR.	18. SUBJECT TERMS (Continue on reverse if necessary and identify by block number)

19. ABSTRACT (Continue on reverse if necessary and identify by block number)

The necessary relationships and a calibration procedure is presented for a rotating analyzer infrared ellipsometer that uses wire grid polarizing optics. The wire grid polarizers contribute signficant ellipticity due to relatively low extinction ratios. Jones matrices are used for the quarter-wave-plate, polarizer, sample, rotating analyzer ellipsometer configuration. Results from a calibrated infrared and visible light ellipsometer for silicon dioxide films on silicon are compared.

20. DISTRIBUTION/AVAILABILITY OF ABSTRACT UNCLASSIFIED/UNLIMITED ☒ SAME AS RPT. ☐ DTIC USERS ☐	21. ABSTRACT SECURITY CLASSIFICATION Unclassified
22a. NAME OF RESPONSIBLE INDIVIDUAL Dr. Mark Ross	22b. TELEPHONE NUMBER (Include Area Code) (202) 696-4410 22c. OFFICE SYMBOL

DD FORM 1473, 83 APR EDITION OF 1 JAN 73 IS OBSOLETE

Infrared rotating analyzer ellipsometry: calibration and data processing.

V.A.Yakovlev*, M.Li and E.A.Irene
Department of Chemistry
University of North Carolina at Chapel Hill
Chapel Hill, NC 27599-3290

* Institute of Crystallography, Acad. of Sci. of the USSR,
Leninsky pr., 59 Moscow 117333 USSR

Abstract

The necessary relationships and a calibration procedure is presented for a rotating analyzer infrared ellipsometer that uses wire grid polarizing optics. The wire grid polarizers contribute significant ellipticity due to relatively low extinction ratios. Jones matrices are used for the quarter-wave-plate, polarizer, sample, rotating analyzer ellipsometer configuration. Results from a calibrated infrared and visible light ellipsometer for silicon dioxide films on silicon are compared.

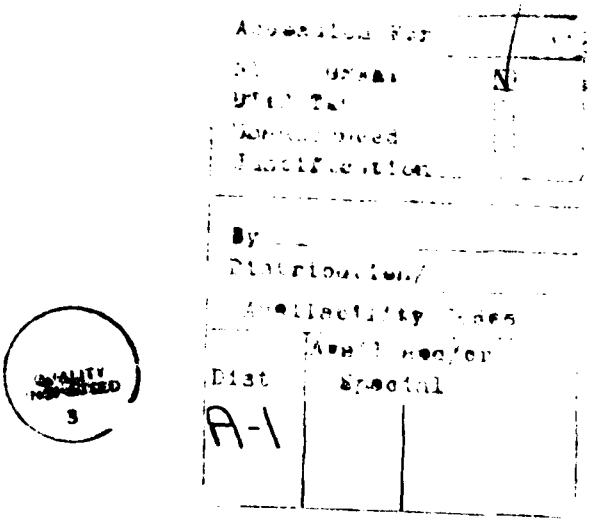

Infrared rotating analyzer ellipsometry: calibration and data processing.

V.A.Yakovlev*, M.Li and E.A.Irene
Department of Chemistry
University of North Carolina at Chapel Hill
Chapel Hill, NC 27599-3290

* Institute of Crystallography, Acad. of Sci. of the USSR,
Leninsky pr., 59 Moscow 117333 USSR

Introduction

Rotating-analyzer ellipsometers (RAE), which use the visible and near-UV spectral range, have become convenient tools with which to study thin films. Infrared ellipsometry has emerged as a powerful complement to visible light ellipsometry (1-5), since a number of advantages are associated with the use of monochromatic IR irradiation. First, with longer wavelengths, IR ellipsometry has a significantly larger ellipsometric period for semiconductor and insulator films. This reduces the uncertainty associated with the measurement of films with thickness greater than an ellipsometric period, D. Because of the periodicity of ellipsometry parameters for films, the measured thickness must be known a priori to ±D. D for 632.8 nm He-Ne laser light for polycrystalline Si, Poly-Si, or amorphous Si, a-Si, is about 80 nm, and for SiO_2, D is about 280

nm. However, for 1.53 μm IR laser radiation the ellipsometric periods are 230 nm and 710 nm, respectively. Second, for an absorbing film, single wavelength visible light ellipsometry suffers from the necessity to accurately know the extinction coefficient, in order to determine the film thickness. The problem is complicated for Poly-Si where the extinction coefficient depends strongly on the film preparation conditions. For optical purposes Poly-Si can be considered to be a mixture of crystalline and amorphous Si (6), with an extinction coefficient, k, varying from $k_{c\text{-}Si}$=0.024 to $k_{a\text{-}Si}$=0.4 for 632.8 nm light. However, for 1.53 μm light $k_{c\text{-}Si}$=0 and $k_{a\text{-}Si}$<0.01. Considering that the refractive indices for c-Si and a-Si are respectively $n_{c\text{-}Si}$=3.478 and $n_{a\text{-}Si}$=3.480 at λ=1.53 μm (7), it is clear that the optical properties of Poly-Si in the IR range are only very slightly dependent on preparation conditions. Thus, if one desires film thicknesses, the IR range is superior.

Ellipsometry theory is well developed for both physical principles and calibration procedures. Calibration procedures for visible light RAE are also well known (8-9). For visible light ellipsometry high quality polarizing optical components are readily available. However, the IR spectral range beyond several μ wavelength requires different polarizing elements. For RAE the polarizing components should be reasonably compact and introduce minimum beam deviation and distortion; in the infrared region, grid polarizes are satisfactory with an average half-angle beam deviation for a gold grid BaF_2 polarizer of less than 0.1 mr. Unfortunately the extinction ratios are not large and therefore

these components act as elliptical polarizers. Consequently, the calibration procedures and data processing that were developed for ellipsometers with more nearly perfect optical elements are not applicable. Also for the grid polarizers, the approaches which were derived for RAE with optical elements having small imperfections (10-12) cannot be used. Although the complexity of using IR elements in ellipsometry has been realized (13-15), detailed calibration and data processing procedures have not been published.

In this paper we describe and demonstrate a new procedure for a calibration and data processing of a single-wavelength IR RAE employing elliptical grid polarizes.

Theoretical Considerations

For the optical analysis of the RAE setup shown in Fig. 1a (laser light source - quarter-wave plate - polarizer - sample - rotating analyzer - detector) we use a 2x2 Jones matrix formulation (16).

Let T_p and T_o be the respective complex transmission coefficients for plane polarized light parallel and orthogonal to the transmission axis of the polarizer. Thus the Jones matrix of an optically inactive polarizer in its transmission-extinction, te, principal frame in normalized form is given as:

$$T_p^{te} = \begin{pmatrix} T_p & 0 \\ 0 & T_o \end{pmatrix} \quad or \quad \begin{pmatrix} 1 & 0 \\ 0 & T_o/T_p \end{pmatrix} \qquad (1)$$

The ratio of the transmission coefficients is a complex number:

$$T_o/T_p = \epsilon_p e^{i\Delta_p} \tag{2}$$

where ϵ_p and Δ_p are real values, ϵ_p is the ellipticity coefficient and Δ_p is the relative phase retardation for the polarizer. From an application of the theory of propagation of microwaves around geometrical discontinuities in waveguides, it has been shown (17) that to a good approximation, one may set the relative phase retardation Δ_p equal to $-\pi/2$ for grid polarizes. Therefore, the grid polarizer matrix becomes:

$$T_p^{te} = \begin{pmatrix} 1 & 0 \\ 0 & -i\epsilon_p \end{pmatrix} \tag{3}$$

A quarter-wave plate (position shown in Fig. 1a) can be used to transform elliptically polarized light into nearly circularly polarized light. A real quarter-wave plate is not perfect, hence we use a general form (16) to describe the polarization state χ_{qo} of light emanating from the quarter-wave plate:

$$\chi_{qo}^{ps} = \frac{\tan\theta_q + i\tan\gamma_q}{1 - i\tan\theta_q\tan\gamma_q} = \chi_q \tag{4}$$

where θ_q and γ_q are angles specifying the ellipse of polarization as

shown in Fig.2 and the superscript ps denotes axes corresponding to the plane of incidence.

The Jones matrix for the polarizer in the ps frame is given as:

$$T_p^{ps} = R(-P)\, T_p^{te}\, R(P) \tag{5}$$

where R(P) is the rotation matrix, P is an angle between the p-axis and transmission axis, t, of the polarizer and can be expressed as:

$$P = P^{sc} - P^{off} \tag{6}$$

where P^{sc} is the polarizer scale reading, and P^{off} is the polarizer offset, i.e. polarizer reading relative to the plane of incidence. Now taking into account that the Jones vector of the light emanating from the polarizer is given by:

$$\bar{E}_{po}^{ps} = T_p^{ps}\, \bar{E}_{pi}^{ps} \tag{7}$$

where

$$\bar{E}_{pi}^{ps} = \bar{E}_{qo}^{ps} = \begin{pmatrix} 1 \\ \chi_q \end{pmatrix} \tag{8}$$

the polarization state χ_{po} of the light emergent from the polarizer is:

$$\chi_{po}^{ps} = \frac{E_{po}^{s}}{E_{po}^{p}} = \frac{(1+i\varepsilon_p)\tan P + \chi_q(\tan^2 P - i\varepsilon_p)}{1 - i\varepsilon_p \tan^2 P + \chi_q(1+i\varepsilon_p)\tan P} \qquad (9)$$

This means that the grid polarizer transforms the incident polarization ellipse with angles θ_q and γ_q into a new ellipse with angles θ_p and γ_p (shown in Fig.2) which are related to the exiting polarization state, χ_{po}^{ps}, as (16):

$$\tan 2\theta_p = \frac{2\,Re(\chi_{po}^{ps})}{1 - |\chi_{po}^{ps}|^2} \;,\; \sin 2\gamma_p = \frac{2\,Im(\chi_{po}^{ps})}{1 + |\chi_{po}^{ps}|^2} \qquad (10)$$

Hence we can describe the grid polarizer as a polarizer with an effective axis of transmission t^{eff} which determines an effective polarizer angle P^{eff} with p-axis given by:

$$P^{eff} = P^{eff}(P, \varepsilon_p, \chi_q) = \theta_p \equiv \overline{P} \qquad (11)$$

The effective ellipticity of the light is:

$$\varepsilon^{eff} = \varepsilon^{eff}(P, \varepsilon_p, \chi_q) = \tan\gamma_p \equiv \overline{\varepsilon}_p \qquad (12)$$

and the exiting light Jones vector in the effective $\bar{t}\bar{e}$ frame is:

$$\overline{E}_{po}^{\bar{t}\bar{e}} = \begin{pmatrix} 1 \\ i\overline{\varepsilon}_p \end{pmatrix} \qquad (13)$$

Thus, there is a non-linear dependence between the polarizer orientation and the orientation of the effective polarizer

transmission axis, t^{eff}. This dependence is determined by both the elliptical coefficient, ϵ_p, of the polarizer and polarization state χ_q of the light exiting from the quarter-wave plate.

Analysis of the state of polarization of the light beam as it propagates through the polarizer-sample-analyzer (PSA) sequence of optical elements can be carried out by combining the effects of the individual elements and the inter-element coordinate transformations in a single Jones matrix. Starting with the Jones vector E_{po} given by eqn(13) for the light exiting from the polarizer, the Jones vector of the light emergent from the analyzer and falling on the detector, E_{ao}, is given by:

$$\overline{E}_{ao}^{te} = T_A^{te} R(A)\, T_s^{ps} R(-\overline{P})\, \overline{E}_{po}^{\overline{te}} \qquad (14)$$

where A is an angle between p-axis and transmission axis, t, of the analyzer. The matrixes for the sample and the grid analyzer, respectively, are:

$$T_s^{ps} = \begin{pmatrix} \tan\Psi\, e^{i\Delta} & 0 \\ 0 & 1 \end{pmatrix}, \quad T_A^{te} = \begin{pmatrix} 1 & 0 \\ 0 & -i\varepsilon_A \end{pmatrix} \qquad (15)$$

The intensity of the light emanating from the analyzer, I_{opt}, within a scaling factor is given by:

$$I_{opt} \propto \left|\overline{E}_{ao}^{te}\right|^2 \qquad (16)$$

Taking into account eqns.(13-16), the optical signal detected by

the IR detector can be written as follows:

$$I_{opt} \sim 1 + \alpha \cos 2A + \beta \sin 2A \tag{17}$$

where

$$\alpha = \eta_A \alpha^c \ , \ \beta = \eta_A \beta^c \tag{18}$$

$$\alpha^c = \frac{\tan^2\Psi\,(\cos^2\overline{P} + \overline{\varepsilon}_p^2 \sin^2\overline{P}) - (\sin^2\overline{P} + \overline{\varepsilon}_p^2 \cos^2\overline{P})}{\tan^2\Psi\,(\cos^2\overline{P} + \overline{\varepsilon}^2 \sin^2\overline{P}) + \sin^2\overline{P} + \overline{\varepsilon}_p^2 \cos^2\overline{P}} \tag{19}$$

$$\beta^c = \frac{\tan\Psi\,[2\overline{\varepsilon}_p \sin\Delta + (1 - \overline{\varepsilon}_p^2)\sin 2\overline{P}\cos\Delta]}{\tan^2\Psi\,(\cos^2\overline{P} + \overline{\varepsilon}_p^2 \sin^2\overline{P}) + \sin^2\overline{P} + \overline{\varepsilon}_p^2 \cos^2\overline{P}} \tag{20}$$

$$\eta_A = (1 - \varepsilon_A^2) / (1 + \varepsilon_A^2) \tag{21}$$

For the RAE experimental configuration, it is necessary to distinguish between the optical signal, I_{opt}, and the electrical signal, I_{el}, which is actually measured and evaluated by the controlling computer. The optical signal is transformed into an electrical signal by the detector and then passes through a noise reducing filter (Fig.1b), that introduces a phase shift, φ, and a relative attenuation, η^{el}, of the ac component of the signal with respect to the ac component of the light intensity, which are both dependent upon the analyzer rotation frequency, ω_A. If the detector

response is a linear function of the total light flux impinging upon it, the detector output will be proportional to the intensity of the light exiting the analyzer, I_{opt}, and the electrical signal from the detector, $I_{el}(t)$, is given within a scaling factor by:

$$I_{el}(t) = 1 + \eta^{el}\alpha\cos[2A(t) - \varphi] + \eta^{el}\beta\sin[2A(t) - \varphi] \qquad (22)$$

The signal actually measured, $I_{el}^{ex}(t)$, can be written as:

$$I_{el}^{ex}(t) = 1 + \alpha^{e}\cos 2\omega_A t + \beta^{e}\sin 2\omega_A t \qquad (23)$$

where α^e and β^e are normalized Fourier coefficients (4). Taking into account that $A(t)=w_A t-A^{off}$, where A^{off} is the analyzer offset, i.e. the analyzer reading relative to the plane of incidence, and in comparison with eqns. (22) and (23), the coefficients are written as:

$$\begin{aligned} \alpha^e &= \eta\,(\alpha^c\cos 2A^o - \beta^c\sin 2A^o) \\ \beta^e &= \eta\,(\alpha^c\sin 2A^o + \beta^c\cos 2A^o) \end{aligned} \qquad (24)$$

where

$$\eta = \eta^{el}\eta_A\ ,\ A^o = A^{off} + \varphi \qquad (25)$$

In summary, the derived formulas eqns. (6), (9-12), (19-20), and (21) give the necessary relationships between the polarization state χ_q of the light that impinges upon the polarizer, the polarizer scale reading P^{sc}, the polarizer ellipticity coefficient

ϵ_p, the calibration parameters P^{off}, A°, η, the ellipsometri angles ψ, Δ and the experimentally measured Fourier coefficients α^e, β^e.

Experimental

The IR ellipsometer used in this study is a home built rotating analyzer, single-wavelength ellipsometer with the configuration shown in Fig. 1a. The optical bench has a precision of $\pm 0.02^0$ in the angle of incidence. A He-Ne laser operating at λ=1.53 μm is used as IR light source. A quarter-wave plate is then used to change the linearly polarized light from the laser to circular polarization. Barium fluoride gold grid polarizers are used for both for the polarizer and analyzer. The analyzer is rotated at 5 Hz. The path of the light beam and plane of incidence is determined by a four iris assembly. A liquid nitrogen cooled InSb photovoltaic detector is used to measure the intensity of the IR light. The detector is thermally isolated from short term ambient temperature fluctuations by a form fit foam insulation housing. The detector is stable for about two hours after liquid nitrogen filling. Another He-Ne laser with visible light at 632.8nm is mounted on the polarizer arm for alignment of each optical component and the optical path.

The balance circuit shown in fig.1b is used in between the low-noise preamplifier and voltage follower. When there is no light impinging on the detector, the signal from the ambient is zeroed by this balance circuit which prevents amplifier saturation. Before each measurement the background level (when the light source is

blocked) is determined and subtracted from the measured signal. Thus any small residual analog circuit imbalance is eliminated and the influence of the surrounding thermal radiation becomes negligible.

Calibration Procedure

The goals of the calibration procedure are: first, to determine the polarization state, χ_q, of the light that impinges upon the polarizer; second, to determine plane of incidence, i.e. to find polarizer reading P^{off} relative to the plane of incidence; third, once the plane of incidence is known, to find the coefficient of ellipticity of the polarizer, ϵ_p, and the calibration parameters, A^o, (which is close to the analyzer offset) and η (See eqn.(25)). These goals are reached with the following procedural steps.

1. With the polarizer and analyzer arms in the straight-through configuration the procedures a) through c) are performed.

a. The components: Laser(L) - Polarizer(P) - Rotating analyzer(RA) - Detector(D) are mounted on the optical bench. The polarizer has to be positioned so that its transmission axis is close to the plane of incidence, i.e. $P \approx 0$. By rotating the laser around its axis, the position which gives the maximum amplitude of the modulated signal, is found. At this position the polarization axis of the light from the laser is coincident with the transmission axis of the polarizer.

b. The components: L - Quarter-wave plate($\lambda/4$) - RA - D are mounted

on the optical bench. By rotation of the quarter-wave plate, the setting, C^{∞}_{o}, which gives the minimum deviation of the modulated signal, is found. At this position the light impinging upon the polarizer has a polarization close to circular, i.e. $\tan\gamma_q \approx 1$. Taking into account step a., one of the axes of the ellipse of polarization nearly coincides with the plane of incidence, i.e. $\theta_q = 0$.

c. With the components: L - $\lambda/4$ - RA - D mounted on the optical bench and with $\theta_q = 0$ and $\chi_{qo} = i\tan\gamma_q$ (from eqn.(4)), the detected signal is:

$$I(t) \sim (1+\varepsilon_A^2\tan^2\gamma_q)\cos^2 A(t) + (\varepsilon_A^2+\tan^2\gamma_q)\sin^2 A(t) \qquad (26)$$

Taking into account, that $\tan\gamma_q \approx 1$, i.e. $\tan\gamma_q = 1-\delta$, where $\delta << 1$ and that $\varepsilon_A < 1$, the first-order approximation yields:

$$I(t) \sim 1-2\delta\sin^2 A(t) \qquad (27)$$

Hence δ is equal to a half-amplitude of the normalized electrical signal deviation at the L - $\lambda/4$ - RA - D configuration. Thus, the polarization state $\chi_q = i\tan\gamma_q = i(1-\delta)$ is determined.

2. In order to determine the plane of incidence, we use a slightly modified residue calibration technique which is well-developed for RAE (3-5). The main difference when applied to an ellipsometer with grid polarizers is that the polarizer te frame is

replaced by the effective $\bar{t}\bar{e}$ frame which forms an angle P^{eff} with the plane of incidence (Fig.2). Hence the residue $R(P^{eff})$ is given by:

$$R(P^{eff}) = 1 - (\alpha^e)^2 - (\beta^e)^2 \tag{28}$$

In this case the residue calibration is accomplished by measuring the residue $R(P^{eff})$ at a number of equidistant polarizer settings near $P^{eff} \approx 0$ instead of measuring the residue R(P) in the vicinity of P^{eff}, i.e. at $P \approx 0$. First P^{eff} can be roughly estimated at the Brewster angle position by using a transparent sample (16). With this configuration, the polarizer setting is found which gives minimum intensity of the reflected beam. At this setting the effective transmission axis of the polarizer is oriented nearly parallel to the plane of incidence, i.e. $P^{eff} \approx 0$. Then by the residue calibration, we can precisely find the polarizer setting at which the residue is a minimum and thus the effective transmission axis coincides with the plane of incidence, i.e. $P^{eff} = 0$. The sample with $\Delta \approx \pi/2$ is the best choice for this procedure (8), since with Δ near $\pi/2$ the curvature of the residue $R(P^{eff})$ in the vicinity $P^{eff} \approx 0$ is large, enabling one to determine the minimum R with a high degree of accuracy. From the condition $P^{eff} = 0$, which is reached at minimum residue, it follows that:

$$Re\,[\chi_{po}^{ps}(P^{\circ})] = 0 \tag{29}$$

where P° is a polarizer angle at which the residue is minimal and

eqn. (29) is satisfied. From the eqn.(9), taking into account that $\tan P^* \sim \epsilon_p$ (as will be shown below) and $\tan P^* < 1$, neglecting the term $\tan^3 P^*$, and with $\tan^4 P^* << 1$, we obtain the relation:

$$\tan P^* = \frac{\epsilon_p Re(\chi_q)}{\epsilon_p^2 \tan^2 \gamma_q - 1} \qquad (30)$$

Using two settings of the quarter-wave plate $C_1 = C^{sc}_o$ and $C_2 = C^{sc}_o + \pi/2$ with corresponding angles P_1^* and P_2^*, we can nearly achieve right and left circularly polarized light impinging upon the polarizer, i.e. $\chi_{q1}(C_1) = i\tan\gamma_q$ and $\chi_{q2}(C_2) = -i\tan\gamma_q$. Thus, $P_1^* = -P_2^*$. From eqn.(6) $P_1^* = P_1^{sc} - P^{off}$ and $P_2^* = P_2^{sc} - P^{off}$, and therefore:

$$P^{off} = \frac{1}{2}(P_1^{sc} + P_2^{sc}) \,, \quad \epsilon_p = \frac{1}{2\tan\gamma_q}(\tan P_1^* - \tan P_2^*) \qquad (31)$$

where P_1^{sc} and P_2^{sc} are the polarizer scale readings corresponding to two minimums of the residues, which are measured at quarter-wave settings C_1 and C_2, respectively.

Thus, both the plane of incidence, which is determined by the angle P^{off}, and the coefficient of the polarizer ellipticity ϵ_p are known.

3. To find the calibration parameter A^o, which characterizes both the analyzer offset, A^{off}, and the electrical phase shift, φ, the same configuration is used. From eqn. (24) we have:

From the condition $P^{off} = 0$, and taking into account eqns. (19-20)

$$A^{o} = \frac{1}{2}\left(\arctan\frac{\beta^{e}}{\alpha^{e}} - \arctan\frac{\beta^{c}}{\alpha^{c}}\right) \tag{32}$$

we write:

$$\frac{\beta^{c}}{\alpha^{c}} = \frac{2\bar{\varepsilon}_{p}\tan\Psi\sin\Delta}{\tan^{2}\Psi - \bar{\varepsilon}_{p}^{2}} \tag{33}$$

and in accordance with eqn. (9), we arrive at:

$$\bar{\varepsilon}_{p} \sim Im(\chi_{po}^{ps}) \sim \tan P \tag{34}$$

Since it was shown that $P_1^{\bullet} = -P_2^{\bullet}$, then:

$$\varepsilon_{p}(P_1^{sc}) = -\varepsilon_{p}(P_2^{sc}) \tag{35}$$

In order to obtain A^{o}, we define:

$$A_{1,2} = \frac{1}{2}\arctan\left[\frac{\beta^{e}}{\alpha^{e}}\right]_{P_{1,2}^{sc}} \tag{36}$$

where the index 1 or 2 denotes that the experimental values α^{c} and β^{e} are measured at polarizer setting P^{sc}_1 or P^{sc}_2, respectively, and from eqns.(32-36) the result is:

$$A^{o} = \frac{1}{2}(A_1 + A_2) \tag{37}$$

4. To obtain the calibration parameter η, which characterizes both the relative amplitude attenuation, η^{el}, of the electrical

signal and the analyzer ellipticity, ϵ_A, the straight-through configuration was used. With this configuration the residue R(P) is given as:

$$R(P) = 1-\eta\left[\frac{1-\overline{\epsilon}_p^2(P)}{1+\overline{\epsilon}_p^2(P)}\right]^2 \qquad (38)$$

Taking into account that at $\theta_q = 0$ (which is reached at the first step of the calibration) and at P = 0 it follows from eqns.(9) and (10), that $\epsilon_p = 0$, and the residue $R(0) = 1-\eta^2$. Hence using the orientation of the polarizer P = 0 we can determine η as:

$$\eta = \sqrt{1-R(0)} \qquad (39)$$

Data Reduction

Because of the nonlinearity of eqns. (19-20) and (24) which describe relations between experimentally measured normalized Fourier coefficients α^e and β^e and the ellipsometric angles ψ and Δ, it is impossible to determine ψ and Δ from α^e and β^e by an analytical inversion. The direct use of α^e and β^e to find the unknown parameters for a thin film system improves the precision, since α^e and β^e are the first results calculated from experimentally measured intensity data as a function of analyzer angle. Furthermore, the Fourier coefficients have the same weight and range as ψ and Δ (18).

To improve precision and reduce intercorrelation between unknown parameters, measurements at multiple angles of incidence ϕ_i (19) in the range 65-80°, were used. A modelling procedure was used that utilized a minimization of the difference between experiment and calculation using eqns. (19-20) and (24) (with an intermediate calculation of the useful ellipsometric variables ψ and Δ).

In order to find unknown parameters of the modeled thin film structure, we used the Marquardt non-linear best-fit algorithm which minimizes the value of the error function:

$$Q=\sum_i \left[(\alpha^e_{ical}(\phi_i, U) - \alpha^e_{iexp})^2 + (\beta^e_{ical}(\phi_i, U) - \beta^e_{iexp})^2 \right] \qquad (40)$$

where $U=(u_1, u_2, \ldots, u_N)$ is a vector of N unknown film and substrate parameters and ϕ_i is the angle of incidence. Subscripts cal and exp refer to calculated and experimentally derived values.

The program returns the vector U when an initial guess, U_0, is given as input, i.e. the program returns a value of U at the local minimum of Q, near the initial value. In addition, correlation between all fitting parameters are expressed in terms of the correlation matrix of the derivatives $\partial\alpha/\partial u_n$, $\partial\beta/\partial u_n$ and a 95% confidence limit was used to calculate errors in the parameters.

Experimental Results

To calibrate the optical system, a thermally grown SiO_2 film on Si was used with a thickness 119.8 nm and refractive index 1.465, as was measured by a high precision null-type ellipsometer at ϕ=70°.

This sample yields $\Delta \approx 90°$ and $\psi \approx 21°$ at $\phi \approx 70°$ at 1.53μm IR irradiation, and also there is large curvature of the residue, thereby enabling the calibration of parameters with high accuracy. Following the procedures described above, we obtained the ellipticity of the polarizer $\epsilon_p = 0.23$, $\eta_A = 0.845$ (which corresponds to an ellipticity of the analyzer $\epsilon_A \approx 0.29$, taking into account that $\eta^{el} \approx 1$ at the low frequency, $\omega_A = 5$Hz, of the analyzer rotation). This ellipticity of the polarizer transforms the polarizer transmission axis into an effective transmission axis, which yields an effective polarizer angle $P^{eff} \approx 12°$ at a polarizer azimuth P=0.

As a demonstration of the procedures, the thickness of the SiO_2 sample was measured using multiple angles of incidence from 67° to 73° with a result of 118.2 nm ± 5 nm in substantial agreement and within 1% of the result obtaineed with visible light ellipsometry. Fig. 3a and b show the comparison of Ψ and Δ versus angle of incidence ϕ, where Ψ_{cal} and Δ_{cal} were calculated for SiO_2 with thickness 118.2 nm. Additionally, a two layer structure composed of a Si substrate, an SiO_2 film and Poly-Si film overlayer was measured and we obtained a precision in the film thickness of better than a few percent.

Conclusions

Explicit expressions have been derived for the Fourier coefficients of the output signal of an IR RA ellipsometer with grid polarizers. The expressions are suitable for practical use and incorporate the effect of the ellipticity of grid polarizers.

Procedures to calibrate an IR ellipsometer with grid polarizers have been presented along with a data reduction procedure. Experimental verification confirmed high accuracy for the proposed approach.

Acknowledgements

This research was supported in part by the Office of Naval Research, ONR.

References.

1. A.R.Hilton and C.E.Jones, "Measurement of epitaxial film thickness using an infrared ellipsometer", J.Electrochem.Soc., 113,472 (1966).

2. J.D.Fedyk, P.Mahaffy and M.J.Dignam, "Application of IR ellipsometric spectroscopy to surface studies", Surf.Sci., 89,404 (1979).

3. R.T.Graf, J.L.Koenig and H.Ishida, "Fourier transform infrared ellipsometry of thin polymer films", Anal.Chem.,58,64 (1986).

4. F.Ferrieu, "Infrared spectroscopic ellipsometry using a Fourier transform infrared spectrometer: Some applications in thin-film characterization", Rev.Sci.Instrum., 60,3212 (1989).

5. N.Blayo and B.Drevillon, "Interaction between growing amorphous silicon and glass substrate evidenced by in situ infrared ellipsometry", Appl.Phys.Lett., 57,786 (1990).

6. E.A.Irene and D.W.Dong, "Ellipsometry measurements of polycrystalline silicon films", J.Electrochem.Soc. 129,1347 (1982).

7. E.D.Palik, Ed., Handbook of Optical Constants of Solids (Academic,New York,1985).

8. D.E.Aspnes and A.A.Studna, "High precision scanning ellipsometer", Appl.Opt. 14,220 (1975).

9. J.M.M.de Nijs et al., "Calibration method for rotating-analyzer ellipsometers", J.Opt.Soc.Am.A, 5,1466 (1988).

10. D.E.Aspnes, "Effects of component optical activity in data reduction and calibration of rotating-analyzer ellipsometers", J.Opt.Soc.Am., 64,812 (1974).

11. R.M.A.Azzam and N.M.Bashara, "Analysis of systematic errors in rotating-analyzer ellipsometers", J.Opt.Soc.Am., 64,1459 (1974).

12. J.M.M.de Nijs and A.van Silfhout, "Systematic and random errors in rotating-analyzer ellipsometry", J.Opt.Soc.Am.A, 5,773 (1988).

13. T.A.Leonard et al., "Design and construction of three infrared ellipsometers for thin film research", Opt.Eng., 21,971 (1982).

14. R.W.Stobie, B.Rao and M.J.Dignam, "Automatic ellipsometer with high sensitivity and special advantages for infrared spectroscopy of adsorbed species", Appl.Opt., 14,999 (1975).

15. O.Acher, E.Bigan and B.Drevillon, "Improvements of phase-modulated ellipsometry", Rev.Sci.Instrum.60,65,(1989).

16. R.M.A.Azzam and N.M.Bashara, Ellipsometry and Polarized Light (North-Holland,Amsterdam,1977).

17. R.W.Stobie and M.J.Dignam, "Transmission properties of grid polarizers", Appl.Opt., 12,1390 (1973).

18. S.Y.Kim and K.Vedam, "Proper choice of the error function in modeling spectroellipsometric data", Appl.Opt., 25,2013 (1986).

19. G.H.Bu-Abbud and N.M.Bashara, "Parameter correlation and precision in multiple-angle ellipsometry", Appl.Opt., 17,3020 (1981).

Figure captions

Figure 1a. Schematic representation of the optical components for an IR ellipsometer.

Figure 1b. Schematic representation of the electrical part of the IR ellipsometer.

Figure 2. Schematic representation of the ellipse of polarization transformation by a grid polarizer.

Figure 3a, b. The angle of incidence dependencies of the calculated ellipsometrical angles ψ_{cal} and Δ_{cal} in comparison with the experimental points.

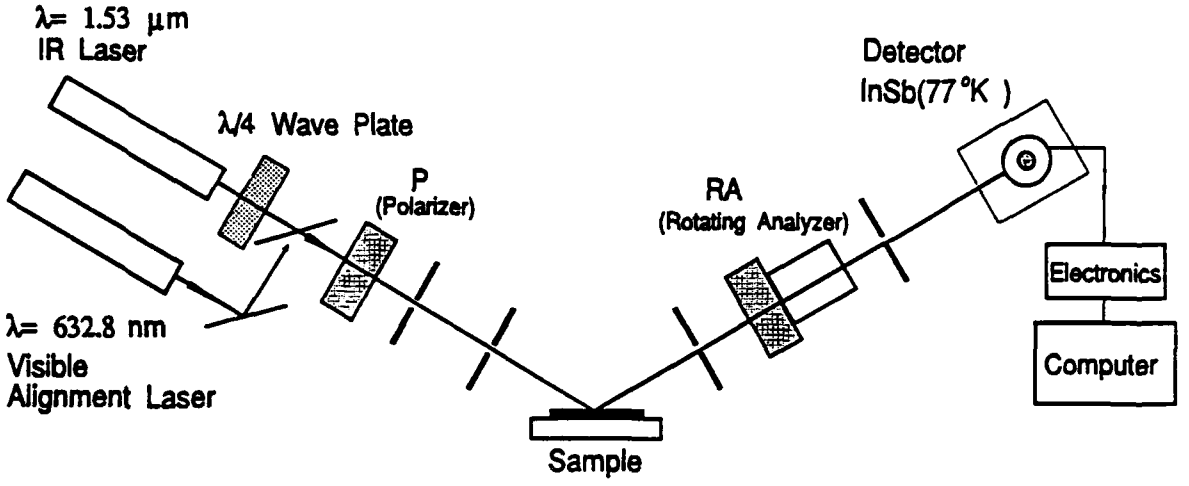
λ= 1.53 μm
IR Laser
λ/4 Wave Plate
P
(Polarizer)
λ= 632.8 nm
Visible
Alignment Laser
Sample
RA
(Rotating Analyzer)
Detector
InSb(77°K)
Electronics
Computer

Fig. 1a

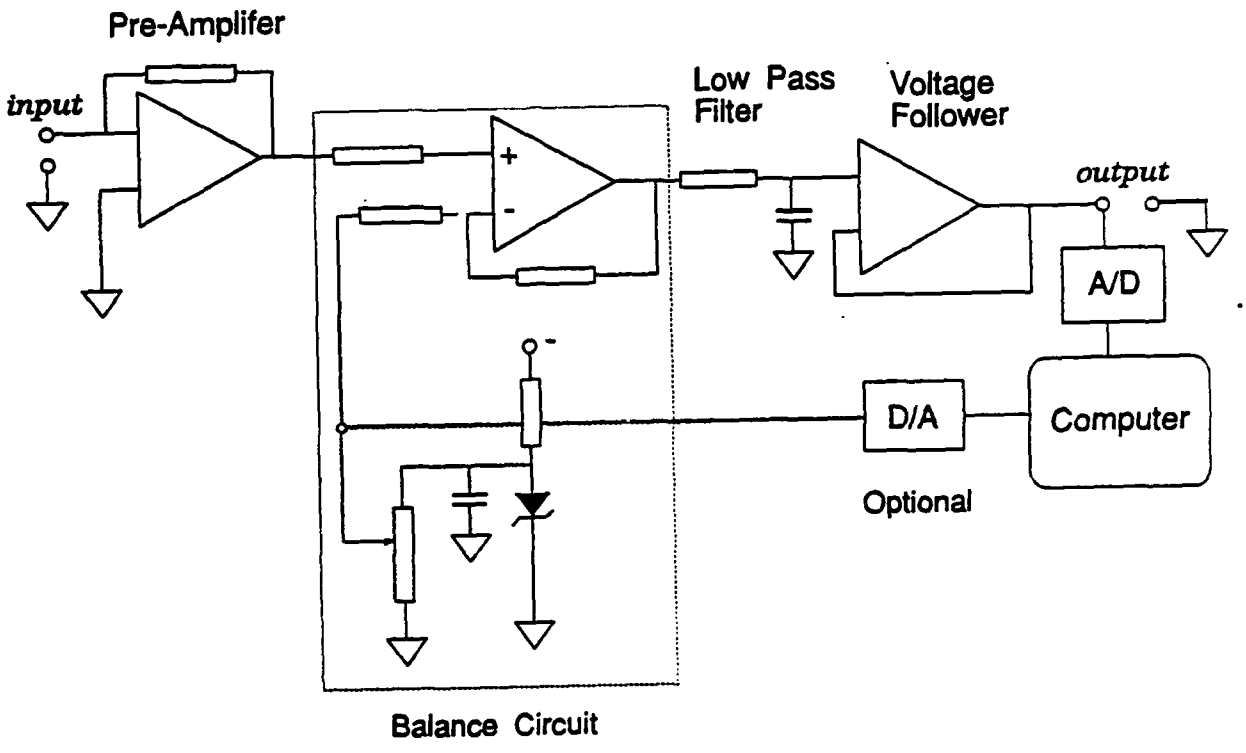
Pre-Amplifer
input
Low Pass
Filter
Voltage
Follower
output
A/D
D/A
Computer
Optional
Balance Circuit

Fig. 1b

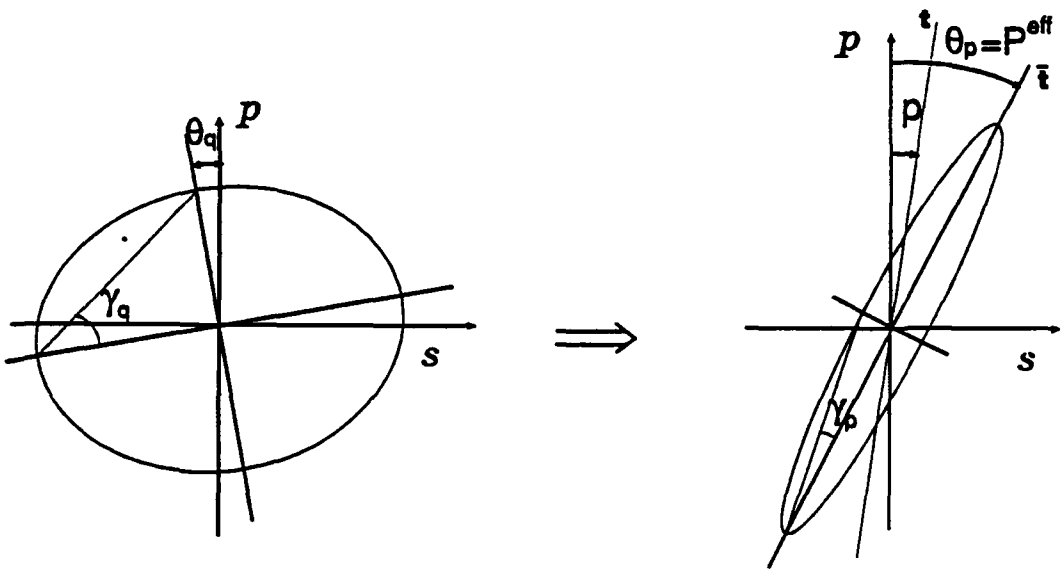

Fig. 2

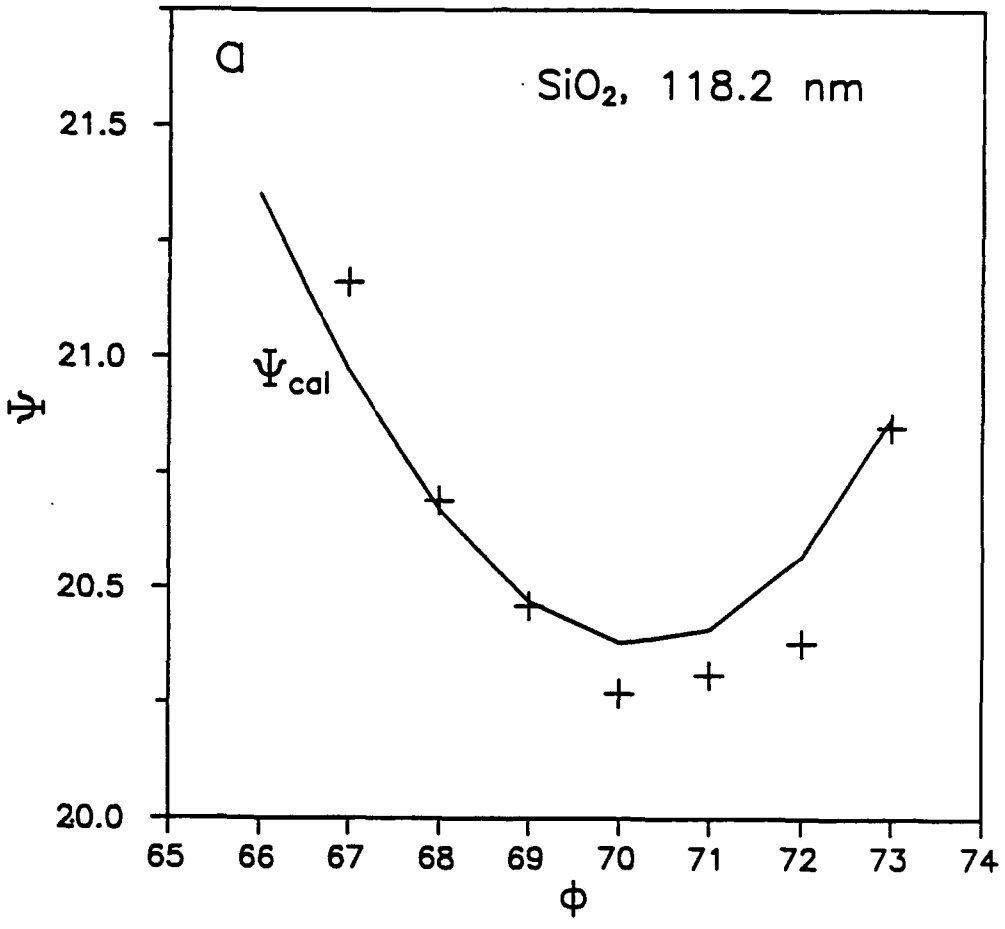
a
SiO_2, 118.2 nm
21.5
21.0
20.5
20.0
Ψ
Ψ_{cal}
65
66
67
68
69
70
71
72
73
74
Φ

Fig. 3a

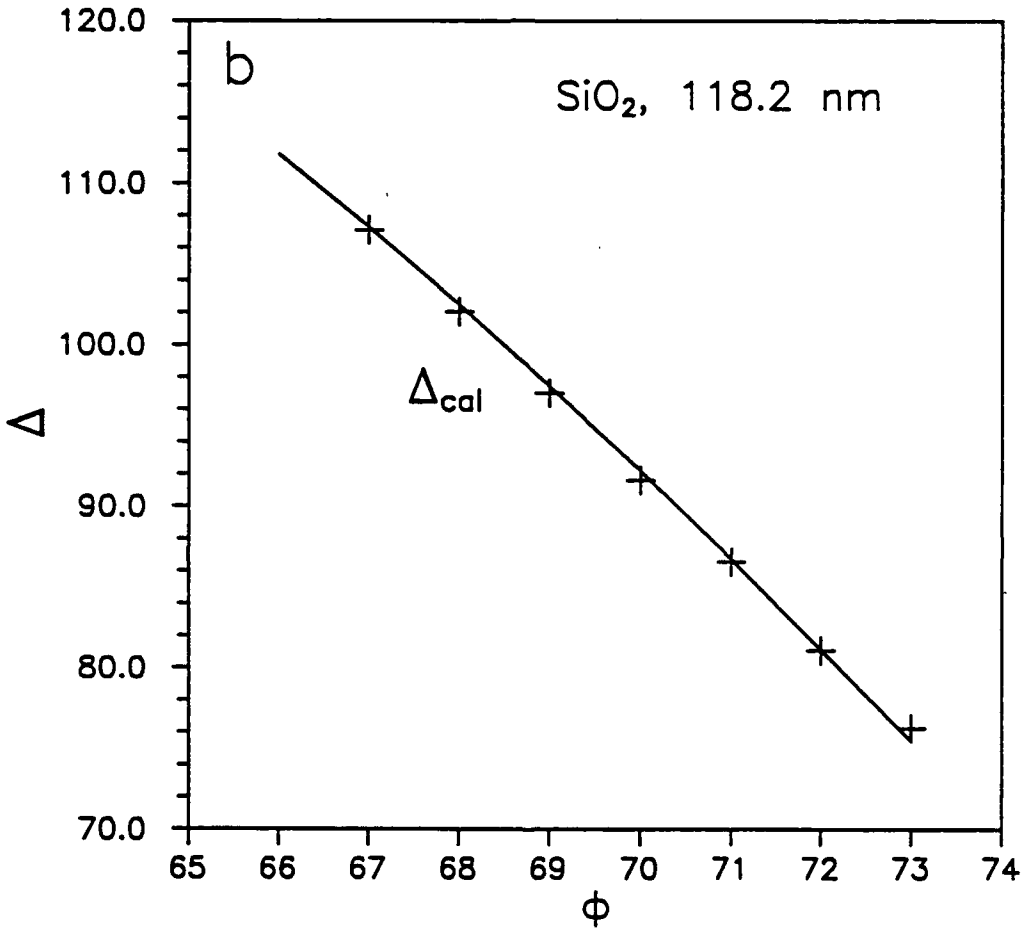
b
SiO_2, 118.2 nm
Δ_{cal}
Δ
Φ
120.0
110.0
100.0
90.0
80.0
70.0
65
66
67
68
69
70
71
72
73
74

Fig. 3b